Modelling and robust control of a soft robot based on conjugated polymer actuators

Amir Ali Amiri Moghadam*, Majid Moavenian and Hamid Ekhteraee Toussi

Faculty of Eng., Department of Mechanical Eng.,
Ferdowsi University of Mashhad,
P.O. Box: 9177948944-11, Mashhad, Iran
E-mail: am_am302@stu-mail.um.ac.ir
E-mail: moaven@um.ac.ir
E-mail: ekhteraee@um.ac.ir
*Corresponding author

Abstract: In this paper, modelling and robust control of a two segment robot arm made from polypyrrole is proposed. Conjugated polymer actuators can be employed to achieve micro and nano scale precision, having a wide range of application including biomimetic robots, and biomedical devices. They can operate with low voltage while producing large displacement, in comparison to robotic joints, they do not have friction or backlash, but on the other hand, they have highly uncertain and time-varying electro-chemo-mechanical dynamics, which makes accurate and robust control of the actuator difficult. This paper consists of two major parts. In the modelling part, first, a suitable dynamic model is developed using Golubev technique, then kinematic modelling of robot is presented. Adaptive neuro-fuzzy inference system (ANFIS) is employed successfully to solve the inverse kinematics problem for different trajectories; this is examined for horizontal line and elliptical trajectories. In the controlling part, the robust control QFT is applied to control the conjugated polymer actuator. Analysis of the design shows that QFT controller has consistent and robust tracking performance.

Keywords: conjugated polymer actuators; polypyrrole; PPy; soft robot; adaptive neuro-fuzzy inference system; ANFIS; uncertainty; quantitative feedback theory; QFT.

Reference to this paper should be made as follows: Amiri Moghadam, A.A., Moavenian, M. and Toussi, H.E. (2011) 'Modelling and robust control of a soft robot based on conjugated polymer actuators', *Int. J. Modelling, Identification and Control*, Vol. 14, No. 3, pp.216–226.

Biographical notes: Amir Ali Amiri Moghadam is currently pursuing his PhD in Mechanical Engineering at Ferdowsi University of Mashhad, Mashhad, Iran. He is a member of the Iranian National Elite Foundation, which is the most prestigious academic honour society in Iran. He is also a Lecturer at the University of Applied Science & Technology, and IAUM (SAMA Branch). His current research interests include robotics, mechanical vibration, robust control, modelling, and control of conjugated polymer actuators for application in micro manipulation systems. He has published over 16 scientific papers in these and related research fields.

Majid Moavenian is currently an Associate Professor of Mechanical Engineering at Ferdowsi University of Mashhad. He completed his BSc in Mechanical Engineering at University of Tabriz (Azarabadegan 1976). He continued his study in Aston University in Birmingham, UK, where he received his pre MSc and MSc (1979). Since then, he joined the organisation for development of rural areas industries. He joined Mechanical Eng. Dept. University of Tehran (1987). Later, he received his PhD from UWCC (UK) on Development of Failure Detection Systems using Luenberger type observers and their application to machines (1993). He was one of the founders of the Mechanical Engineering Society of Khorasan and a member of ISME. His research interests are in the areas of evolutionary system design, dynamic modelling and robust control, application of fuzzy logic and control, soft computing in design of failure and fault diagnosis systems. He has published over 50 peer-reviewed articles in these and related research fields.

Hamid Ekhteraei Toussi started his BSc in Mechanical Engineering at Ferdowsi University of Mashhad (FUM) in February 1984 which continued until March 1988. After that, he worked as a Laboratory Director until January 1990. He carried out his MSc in Mechanical Engineering at the Sharif University of Technology (SUT) in Iran until September 1992 and returned to work in November 1992 as a Lecturer at FUM. From February 1997 to February 2003, he completed his PhD in Mechanical Engineering at SUT. The title of his dissertation is 'EFGM interface crack stress analysis'. Currently, he is working as an Assistant Professor at FUM.

He has supervised more than 30 BSc dissertations, seven MSc dissertations and two PhD students. He is the author of more than 20 journals and conference papers which are available at http://ekhteraee.profcms.um.ac.ir/index.php/publications.

1 Introduction

There is an increasing request for new generation of actuators which can be used in devices such as artificial organs, micro robots, human-like robots and medical applications. Until now, lots of research has been done on developing new actuators such as shape memory alloys, piezoelectric actuators, magnetostrictive actuators, contractile polymer actuators and electrostatic actuators (Hollerbach et al., 1992; Hunter and Lafontaine, 1992). The main disadvantages of these actuators are low efficiency, high electrical power, and low strain generation (Hunter and Lafontaine, 1992). Conjugated polymer actuators seem to be the best solution since they produce reasonable strain under low input voltage.

The main process which is responsible for volumetric change and the resulted actuation ability of the conjugated polymer actuators is reduction/oxidation (RedOx).Thus based on different variety of fabrication forms, different configuration of the actuators can be obtained namely: linear extenders, bilayer benders, and trilayer benders (Della Santa et al., 1997; Smela et al., 1995; Kaneto et al., 1995). By applying a voltage to the actuator, the polypyrrole (PPy) layer on the anode side is oxidised while that on the cathode side is reduced. Ions can transfer inside the conjugated polymer actuators based on two main mechanisms namely diffusion and drift (Madden, 2000). There are many reports in the literature about potential application of electroactive polymer (EPA) in different robotic systems. Bar-Cohen et al. (1998) have presented several EAP driven mechanisms that emulate human hand including a gripper, manipulator arm and surface wiper. Jager et al. (2000) reviewed the current status of micro actuators based on EPA. They described micro fabrication of this actuator plus the possible application of them in micro systems (Jager et al., 2000).

Tadokoro et al. (1999) have presented multi-degree-of-freedom (DOF) micro motion devices based on soft gel actuator (ICPF). Guo et al. (1995) have applied an IPMC actuator for guiding a microcatheter. Nakabo et al. (2005) have described the kinematic modelling of planar multi-DOF soft robot based on polymer gel actuator. They used the Jacobian for purpose of position control without considering the dynamic of actuator (Nakabo et al., 2005).

Application of PID controller for a PPy actuator based on a first order model is presented in Madden (2003). PID and adaptive control approaches based on a first order empirical model are explained in Bowers (2004). In our previous works, we used parallel distributed compensation (PDC) and multi-level fuzzy- quantitative feedback theory (QFT) controller for controlling of PPy actuators based on a third order model (Amiri Moghadam et al., 2009b, Amiri Moghadam and Tootoonchi, 2010). In this paper, we have proposed application of ANFIS for solving the inverse kinematics problem of a two segment soft robot and also position control has been performed while considering its uncertain dynamics, using robust control QFT.

The main objective of the controlling part is to synthesise suitable controller and pre-filter such that, first resulting in a stable closed loop system and secondly being able to track the desired inputs. As mentioned before the uncertainty in the dynamics of actuators is inevitable, therefore application of robust control techniques is essential for achieving high precision. There are two basic methodologies for dealing with the effect of uncertainty in a system namely adaptive control and robust control. In adaptive control design approach, the controller will estimate the system's parameter online and then will tune itself based on these estimates. In the robust control design approach, the controller has a fixed structure which will satisfy the system specifications over the whole range of plant uncertainty. Although adaptive control can be applied to a wider class of problems, the application of robust control will lead to a simpler controller as the structure of controller is fixed requiring no time for tuning (Ge et al., 1998). Thus, the remainder of the paper will be formed as follows:

1 first, the classical model of the actuator will be reviewed and the model will be developed by incorporating uncertainties such as evaporation of solvent into the model
2 the kinematic model will be presented and application of ANFIS to solve the inverse kinematic problem will be described
3 finally, robust controller QFT will be designed for tracking problem.

2 Trilayer PPy actuator

In this paper, as an example of the conjugated polymer actuators, the trilayer PPy actuator will be considered. Figure 1 depicts the trilayer PPy actuator. As the name indicates, the trilayer PPy actuator consists of three layers. The middle layer is porous polyvinylidene fluoride (PVDF) which is used as a storage tank for the electrolyte and on the both sides of it there are polymer layers (PPy) (Wallace and Spinks, 2007; Fang et al., 2008a).

Figure 1 Three-layer PPy actuator

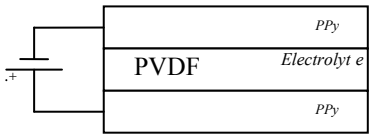

As it has mentioned before, the main process which is responsible for volumetric change of the conjugated polymer actuators is RedOx. Thus in the trilayer bender while the PPy layer on the anode side is oxidised and expands as a result, the PPy layer on the cathode side is reduced and contracts as a result. Therefore this difference in the volume will lead to the bending of the actuator.

3 Electro-chemo-mechanical modelling

The electro-chemo-mechanical model is comprised of two parts, namely electrochemical and electromechanical model.

3.1 Electrochemical modelling

The electrochemical model relates the input voltage and chemical RedOx reaction inside the PPy actuators. Figure 2 depicts the electrical admittance model. For detail description of the equations governing the electrochemical model please refer to (Amiri Moghadam et al., 2009b; Fang et al., 2008b). It is shown that the admittance model $\left(Y(s)=\frac{I(s)}{V(s)}\right)$ of a conjugated polymer in case of single PPy layer is derived as:

$$Y(s)=\frac{s\left[\frac{\sqrt{D}}{\delta}\tanh\left(h\sqrt{s/D}\right)+\sqrt{s}\right]}{\frac{\sqrt{s}}{C}+Rs^{3/2}+R\frac{\sqrt{D}}{\delta}s\tanh\left(h\sqrt{s/D}\right)} \tag{1}$$

where the physical parameters of equation (1) are illustrated in Table 1.

Figure 2 Description of diffusion and double layer charging and its equivalent electrical circuit

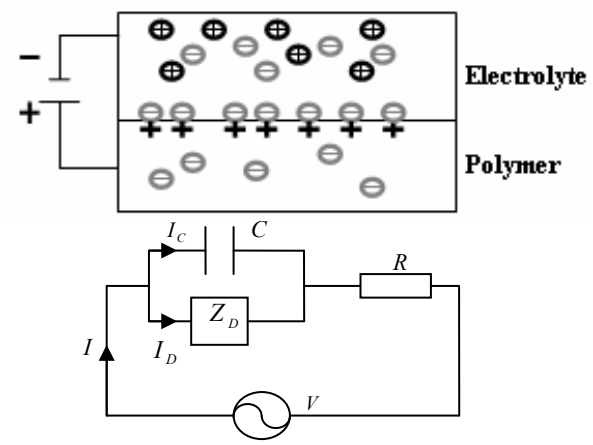

According to Figure 1 in the case of a trilayer bender, the input voltage is applied across double-PPy layers, thus the admittance is half of equation (1) (Fang et al., 2008b).

$$Y(s)_{tri}=\frac{1}{2}.\frac{s\left[\frac{\sqrt{D}}{\delta}\tanh\left(h\sqrt{s/D}\right)+\sqrt{s}\right]}{\frac{\sqrt{s}}{C}+Rs^{3/2}+R\frac{\sqrt{D}}{\delta}s\tanh\left(h\sqrt{s/D}\right)} \tag{2}$$

Table 1 Definition of physical parameters

Parameter	*Definition*
D	Diffusion coefficient
h	Thickness of the PPy layer
R	Electrolyte and contact resistance
δ	Thickness of double-layer capacitance
I	Current
V	Input voltage
C	Double-layer capacitance
Z_D	Diffusion impedance

3.2 Electromechanical modelling

The electromechanical model relates the input voltage and bending displacement of the PPy actuators. It was shown that the relation between the induced in-plane strain (ε) and the density of the transferred charges (ρ) is as below (Otero and Sansinena, 1997):

$$\varepsilon=\alpha.\rho \tag{3}$$

where α is the strain-to-charge ratio. Thus, the induce stress is

$$\sigma=\alpha.E_{PPy}.\rho \tag{4}$$

where E_{PPy} is the Young's modulus of PPy, and ρ can be achieved in the Laplace domain as below (Madden, 2003):

$$\rho(s)=\frac{I(s)}{sWLh} \tag{5}$$

where W is the width and L is the length of the PPy. According to Figure 3, the curvature λ under the induced stress and in the absence of external force is (Madden, 2003):

$$\lambda=\frac{3\alpha}{2h_{pvdf}}.\frac{\left(1+\frac{h}{h_{pvdf}}\right)^2-1}{\left(1+\frac{h}{h_{pvdf}}\right)^3+\frac{E_{pvdf}}{E_{PPy}}-1}.\rho \tag{6}$$

where E_{pvdf} and h_{pvdf} are the Young's modulus and the thickness of the PVDF layer respectively. According to Figure 4 one can obtain the relation between the bending displacement and the curvature as below:

$$x=r.\sin(\theta),y=r.\left(1-\cos(\theta)\right),,\theta=\frac{L}{r}=L.\lambda \tag{7}$$

where x, and y are the bending displacements and θ is the bending angle.

Figure 3 Trilayer PPy actuator

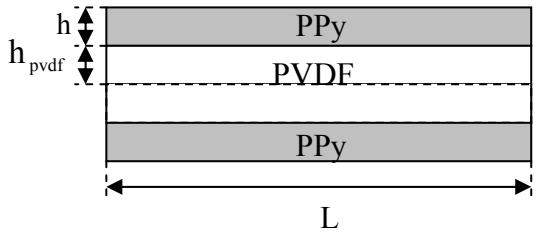

Figure 4 Relation between the bending displacement and the curvature

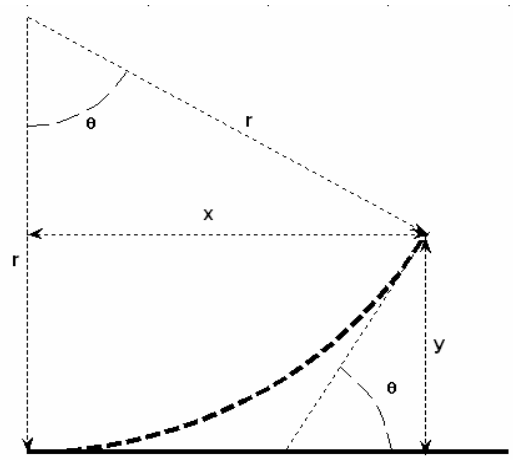

Finally by combining equations (2), (5), (6), and (7) one can obtain the full model between input voltage (V) and output bending angle (θ) as below:

$$\frac{\theta(s)}{V(s)}=\frac{\beta}{sR+\dfrac{1}{C\left(1+\dfrac{\sqrt{D}}{\delta\sqrt{s}}\tanh\left(h\sqrt{\dfrac{s}{D}}\right)\right)}} \tag{8}$$

where

$$\beta=\frac{3\alpha\left[\left(1+\dfrac{h}{h_{pvdf}}\right)^2-1\right]}{4h_{pvdf}hW\left[\left(1+\dfrac{h}{h_{pvdf}}\right)^3+\dfrac{E_{pvdf}}{E_{ppy}}-1\right]} \tag{9}$$

3.3 System identification based on Golubev method

Because the term tanh in equation (8) is not suitable for real time control of the actuator and this equation can not take into account the system uncertainties. Now Golubev method (Golubev and Horowitz, 1982) is used to build a suitable model for control of the actuator. By replacing the term tanh with its equivalent series in equation (8) the actuator model is:

$$\frac{\theta(s)}{V(s)}=\frac{\beta}{sR+\dfrac{1}{C\left(1+\dfrac{2D}{h\delta}\displaystyle\sum_{n=0}^{\infty}\dfrac{1}{s+\pi^2(2n+1)^2D(2h)^{-2}}\right)}} \tag{10}$$

In the first step one can study equation (10) based on its summation term. For this purpose we use the typical values for physical parameters in Table 2 (Fang et al., 2008b).

Thus based on Table 2 and using different values for n [number of terms in equation (10)] one can achieve Table 3.

Based on Table 3, it can be seen that using two terms of equation (10), will lead to a third order system. One zero and one pole of this system are located far to the left of the imaginary axis comparing to the other poles and zeros, thus the system can be reduced to a second order system. Similarly, using three and four terms will lead to third and fourth order systems respectively. Therefore, order of system depends on number of terms, which is used. Thus to solve this problem one can replace the infinite-dimensional system (using tanh) with a family of uncertain linear systems (Torabi et al., 2009). Figure 5 compares the admittance of infinite-dimensional model with its estimation based on two, three, and four terms.

Table 2 Values of physical parameters

Parameter	*Value*
D	$2\times10^{-10}\ m^2/s$
h	30 μm
R	15 Ω
δ	25 nm
C	$5.33\times10^{-5}\ F$
L	$20\times10^{-3}\ m$

Figure 5 Comparisons between using different number of terms and the infinite-dimensional model

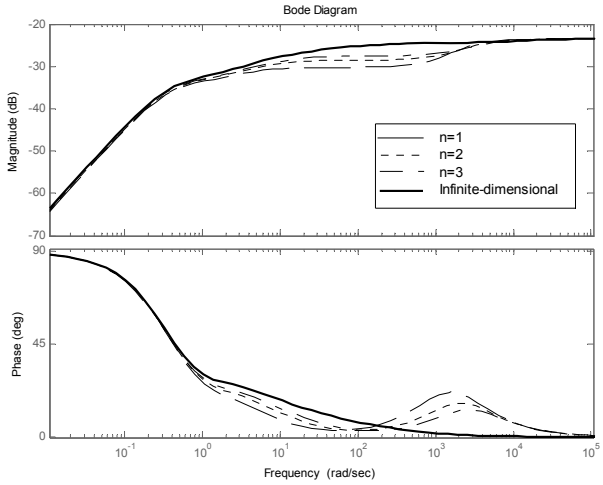

Table 3 The actuator' system poles and zeros based on number of terms used

No. of terms	*Pole*	*Zero*
Two	–0.3793, –3.848, –2,316	–2.736, –1,069
Three	–0.3787, –3.741, –11.47, –2,854	–2.524, –10.25, –1,606
Four	–0.378, –3.696, –11.19, –23.5, –3,391	–2.432, –9.778, –22.29, –2,145

For example the parametric model for using three terms is as below:

$$\frac{\theta(s)}{V(s)} = \frac{a_1 s^3 + a_2 s^2 + a_1 s + a_4}{s^4 + b_1 s^3 + b_2 s^2 + b_3 s + b_4} \tag{11}$$

where

$$Num(s) = \frac{\beta s^3}{R} + \left(\frac{6\beta D}{\delta R h} + \frac{35}{4}\frac{\beta \pi^2 D}{R h^2}\right)s^2 + \left(\frac{35\beta\pi^2 D^2}{\delta R h^3} + \frac{259}{16}\frac{\beta\pi^4 D^2}{R h^4}\right)s + \frac{259}{8}\frac{\beta\pi^4 D^3}{R\delta h^5} + \frac{225}{64}\frac{\beta\pi^6 D^3}{R h^6}$$

$$Den(s) = s^4 + \left(\frac{35}{4}\frac{\pi^2 D}{h^2} + \frac{6D}{\delta h} + \frac{1}{RC}\right)s^3 + \left(\frac{35}{4}\frac{\pi^2 D}{RCh^2} + \frac{35\pi^2 D^2}{\delta h^3} + \frac{259}{16}\frac{\pi^4 D^2}{h^4}\right)s^2 + \left(\frac{259}{16}\frac{\pi^4 D^2}{RCh^4} + \frac{259}{8}\frac{\pi^4 D^3}{\delta h^5} + \frac{225}{64}\frac{\pi^6 D^3}{h^6}\right)s + \frac{225}{64}\frac{\pi^6 D^3}{RCh^6}$$

By using Golubev method for different input signals (sin wave, step…), the uncertain transfer function of admittance model is:

$$\frac{a_1 s^3 + a_2 s^2 + a_3 s}{s^3 + b_1 s^2 + b_2 s + b_3} \tag{12}$$

where

$$a_1 \in [0.05068, 0.06675];\ a_2 \in [1.1, 1.211];\ a_3 \in [2.3, 3.004]$$
$$b_1 \in [25.63, 26];\ b_2 \in [95, 105];\ b_3 \in [35, 45]$$

Application of Golubev method for pulse signal is shown in Figure 6.

Figure 7 depicts the admittance Bode plot for the range of uncertainties associated with equation (12).

In the next step the model will be developed further by considering the effect of actuator resistance and evaporation of the solvent. The actuator resistance is highly depends to the RedOx level (Fang et al., 2008a; Boxall and Osteryoung, 2004). Figure 8 shows the Bode plot of actuator admittance for variation of resistance from 15Ω to 100Ω. Variation of the diffusion coefficient is shown in Figure 9. Therefore by considering the above mentioned uncertainties, and using the Golubev method the uncertain model of the actuator between the input voltage and output bending angle can be achieved as below:

$$\frac{a_1 s^2 + a_2 s + a_3}{s^3 + b_1 s^2 + b_2 s + b_3} \tag{13}$$

where

$$a_1 \in [0.308, 1];\ a_2 \in [5.5, 18.6];\ a_3 \in [15.4, 46.34]$$
$$b_1 \in [25.63, 29];\ b_2 \in [90, 105];\ b_3 \in [20, 45]$$

Thus comparing to the second order LTI model, which was used in Fang et al. (2008b), we develop an uncertain model that can predict the actuator behaviour more accurately. It must be noted that the model reduction process used by Fang et al. (2008b) was based on low frequency application while our model can predict the actuator behaviour in the whole operating frequency range.

Figure 6 System identification based on pulse signal (error = 2.6973e-005)

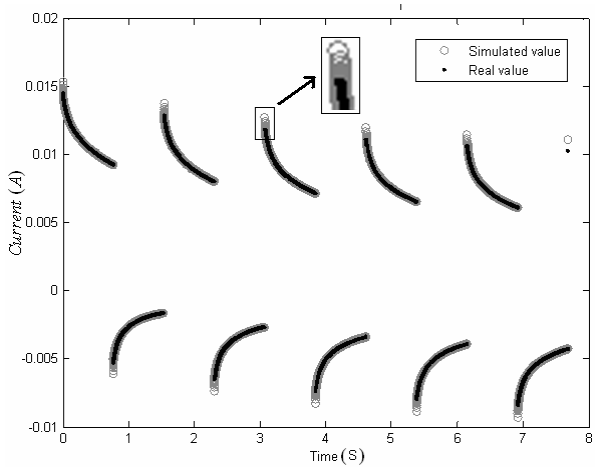

Figure 7 Admittance bode plot based on Golubev method

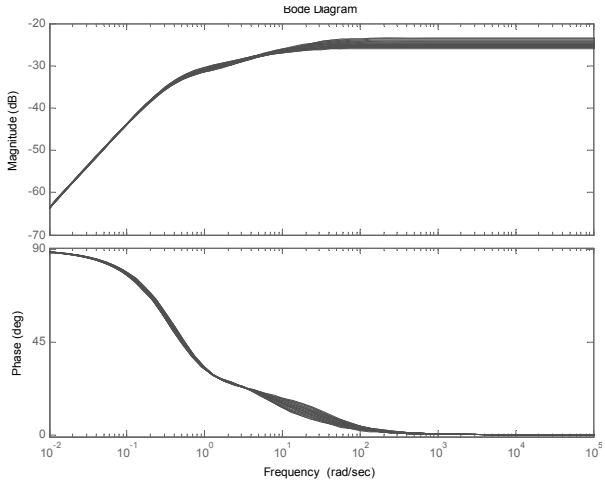

Figure 8 Bode plot of actuator admittance for variation of resistance

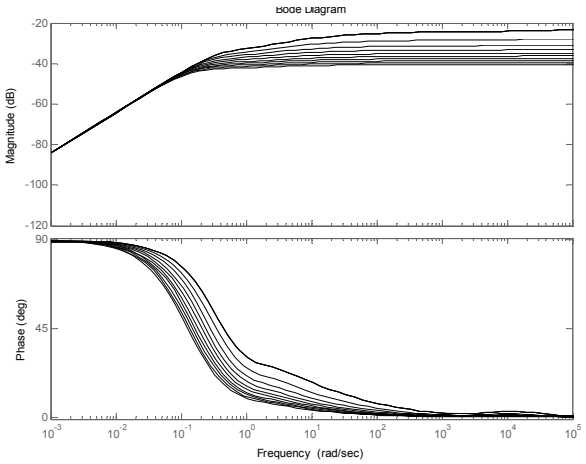

Figure 9 Bode plot of actuator admittance for variation of the diffusion coefficient

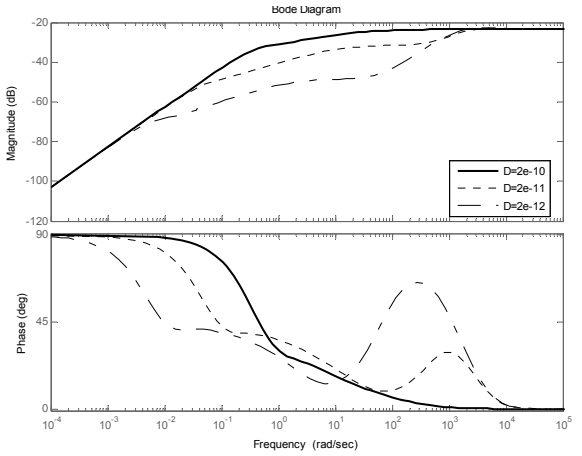

4 Kinematic modelling

4.1 Forward kinematic modelling

In this section, we will present the kinematic model of our soft robot. According to Figure 10, our soft robot is constructed from two identical PPy actuator with physical parameters in Table 2. Kinematic modelling of serial soft robots first proposed in Nakabo et al. (2005). As mentioned in Nakabo et al. (2005), similar modelling approach to conventional serial robot arm manipulator can be used here. Consider the two segment soft robot arm in Figure10. We attached one frame at each joint of the robot and one at the end point of the arm. It is obvious, the transform that defines each frame relative to the previous one consists of a translation equal to the bending displacement (x, y) and a rotation equal to the bending angle (θ). Thus we can define the transform which defines frame $\{i\}$ relative to the frame $\{i-1\}$ as below:

$$ {}^{i-1}_{i}T = \begin{bmatrix} \cos(\theta_i) & -\sin(\theta_i) & r_i \sin(\theta_i) \\ \sin(\theta_i) & \cos(\theta_i) & r_i\left(1-\cos(\theta_i)\right) \\ 0 & 0 & 1 \end{bmatrix} \tag{14} $$

Figure 10 Frame assignment for the soft robot

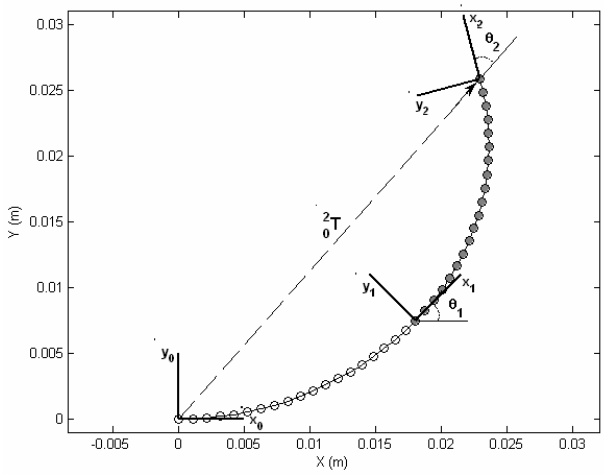

After defining the link frames, one can obtain a single transformation that relates last frame $\{N\}$ to the base frame $\{0\}$ as follow:

$$ {}^{0}_{N}T = {}^{0}_{1}T\,{}^{1}_{2}T\,{}^{2}_{3}T \ldots {}^{N-1}_{N}T. \tag{15} $$

Thus based on equation (15), one can derive the Cartesian position of the last link

$$ \begin{aligned} x &= r_1 \sin(\theta_1) + r_2 \sin(\theta_2)\cos(\theta_1) \\ &\quad - r_2 \sin(\theta_1)\left(1-\cos(\theta_2)\right) \\ y &= r_1\left(1-\cos(\theta_1)\right) + r_2 \sin(\theta_1)\sin(\theta_2) \\ &\quad + r_2 \cos(\theta_1)\left(1-\cos(\theta_2)\right) \end{aligned} \tag{16} $$

Noting that: $r_1 = \dfrac{L_1}{\theta_1}$, and $r_2 = \dfrac{L_2}{\theta_2}$, one can simplify equation (16) as follows:

$$ \begin{aligned} x &= \frac{L_2}{\theta_2}\sin(\theta_1+\theta_2) - \frac{L_2}{\theta_2}\sin(\theta_1) + \frac{L_1}{\theta_1}\sin(\theta_1) \\ y &= -\frac{L_2}{\theta_2}\cos(\theta_1+\theta_2) + \frac{L_2}{\theta_2}\cos(\theta_1) \\ &\quad + \frac{L_1}{\theta_1}\left(1-\cos(\theta_1)\right) \end{aligned} \tag{17} $$

Since the applicability of the robot depends on its workspace. In the next step, we will obtain the workspace of our soft robot.

Given a specific micromanipulation task we can optimise the design of the robot and motion planning based on the robot workspace to satisfy task constraints. According to Figure 11, in order to compute the workspace we vary each joint sequentially between joint limits. Figure 12 shows the workspace of the soft robot while both θ_1 and θ_2 are allowed to vary between ($-\pi$, π) rad.

Figure 11 Motion of the two segment soft robot in its workspace (see online version for colours)

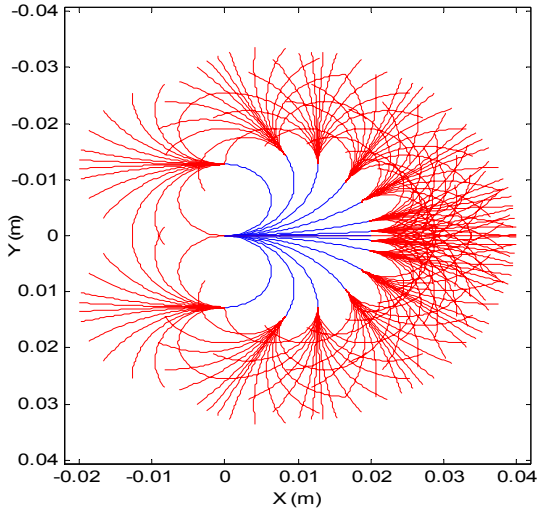

Figure 12 Workspace of a two segment soft robot

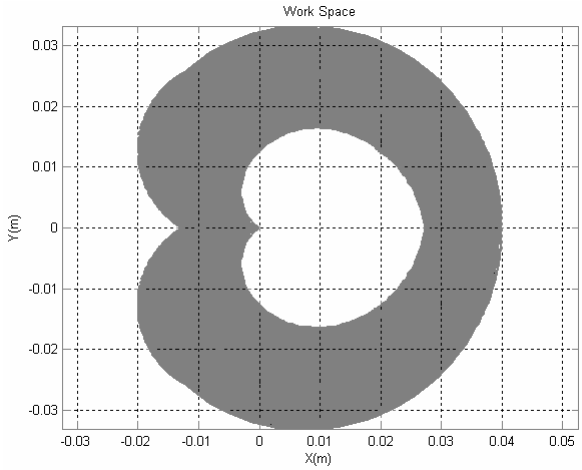

4.2 Inverse kinematic modelling

We must solve the inverse kinematic problem for the purpose of position control. However, it is quite difficult to solve the equation (17); therefore, we propose application of ANFIS for solving the inverse kinematic problem. So far ANFIS has been successfully applied to many practical problems (for example, see Awadallah and Soliman, 2008; Singh and Gill, 2009). The acronym ANFIS derives its name from adaptive neuro-fuzzy inference system (ANFIS). The neuro-adaptive learning method works similarly to that of neural networks. Neuro-adaptive learning techniques provide a method for the fuzzy modelling procedure to learn information about a data set (Jang and Sun, 1997). The parameters associated with the membership functions changes through the learning process. The computation of these parameters (or their adjustment) is facilitated by a gradient vector. This gradient vector provides a measure of how well the fuzzy inference system is modelling the input/output data for a given set of parameters. When the gradient vector is obtained, any of several optimisation routines can be applied in order to adjust the parameters to reduce some error measure. This error measure is usually defined by the sum of the squared difference between actual and desired outputs. ANFIS uses either back propagation or a combination of least squares estimation and back propagation for membership function parameter estimation (Jang and Sun, 1997; Jang, 1993).

In this part of the study, an ANFIS algorithm, developed under MATLAB fuzzy logic toolbox, will be applied. The designed ANFIS system is consisted of two inputs, which are the Cartesian position of the last link and the output is the bending angle of each joint (Figure13). Figure 14 illustrates the training data plus an elliptical path, which will be used to validate the ANFIS model.

Fuzzy membership function for the first input is shown in Figure 15. Structure of the ANFIS model for the first joint is depicted in Figure 16.

Figure 13 ANFIS model of inverse kinematic problem

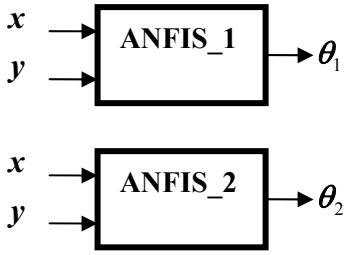

Figure 14 ANFIS training data plus an elliptical path

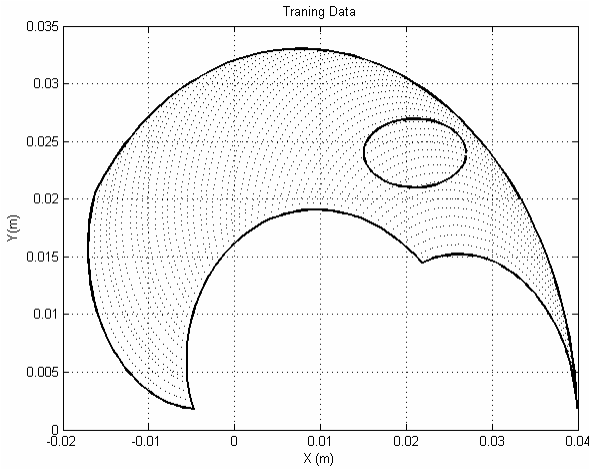

Figure 15 Membership functions

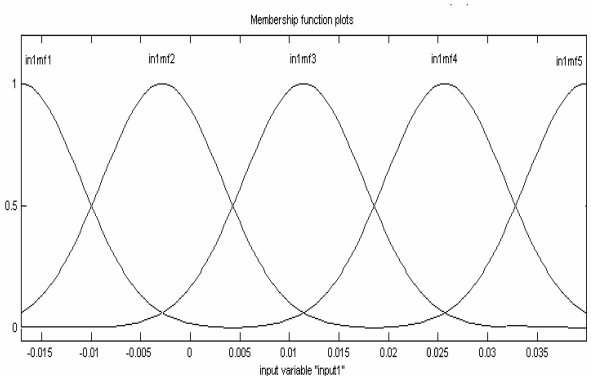

Figure 16 Structure of the ANFIS model (see online version for colours)

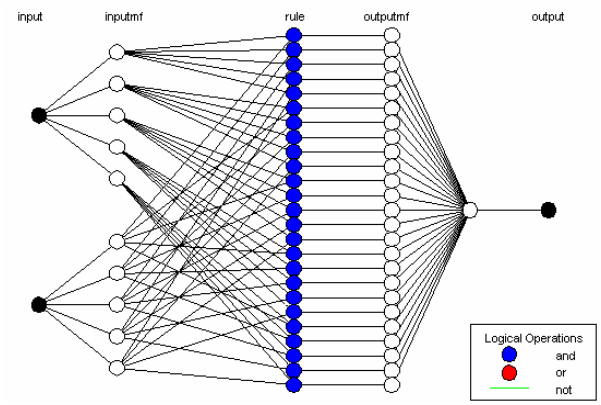

ANFIS output surface based on its inputs for the first joint is shown in Figure 17.

Figure 17 ANFIS output surface based on inputs 1 and 2 (see online version for colours)

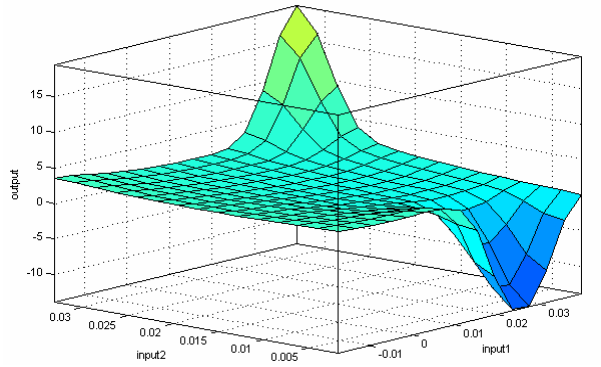

Results obtained by ANIFS for an elliptical, and a horizontal line trajectories are depicted in Figures 18, 19 respectively.

The obtained results indicate that the ANFIS model can greatly predict the suitable bending angle for each joint, so the soft robot can follow the given trajectories.

Figure 18 Results obtained by ANIFS for an elliptical trajectory

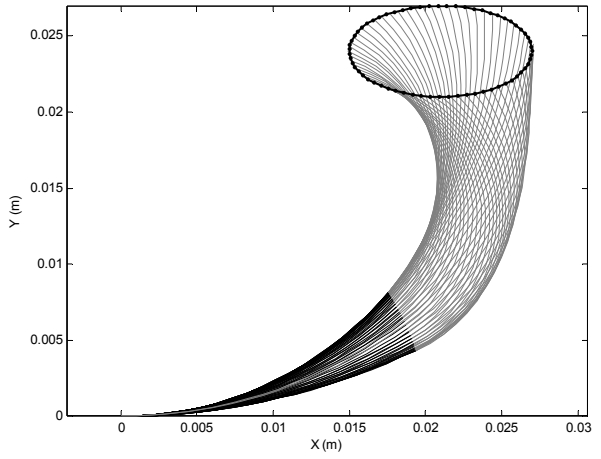

Figure 19 Results obtained by ANIFS for a horizontal line trajectory

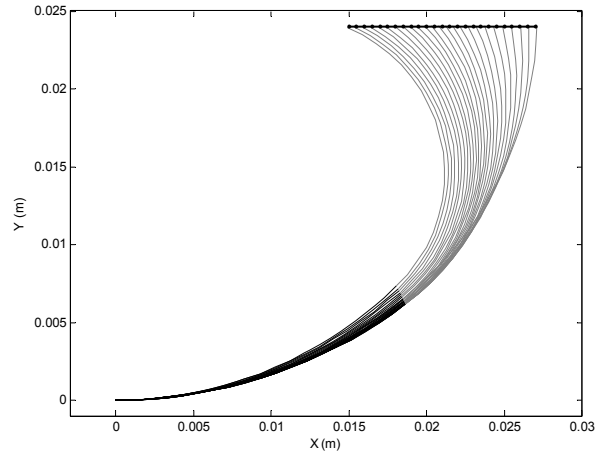

5 Application of quantitative feedback theory (QFT)

There are many practical systems that have high uncertainty in open-loop transfer functions which makes it very difficult to have suitable stability margins and good performance in command following problems for the closed-loop system. Therefore a single fixed controller in such systems is found among 'robust controllers' family. QFT is a robust feedback control-system design technique which allows direct design to closed-loop robust performance and stability specifications. Since then this technique has been developed by him and others (Horowitz and Sidi, 1972; Horowitz, 1992; Houpis, 1995).

In many techniques from 'robust control' family such as H_∞, design is based on magnitude of transfer function in frequency domain, but QFT is not only concerned with aforementioned subject, but also able to take into account phase information in the design process. The unique feature of QFT is that the performance specifications are expressed as bounds on frequency-response loop shapes in such a way that satisfaction of these bounds imply a corresponding approximate closed-loop satisfaction of some time-domain response bounds for given classes of inputs and for all uncertainty in a given compact set. Consider the feedback system shown in diagram Figure 20. This system has the two-degrees of freedom structure [consider controller G(s) and prefilter F(s)]. In this diagram, P(s) is uncertain plant belongs to a set $P(s) \in \{P(s,\varphi); \varphi \in \Phi\}$ where here φ is the vector of uncertain parameters, which takes the values in Φ. G(s) is the fixed structure feedback controller, F(s) is the prefilter and D(s) is the disturbance.

Figure 20 Two degree of freedom feedback system

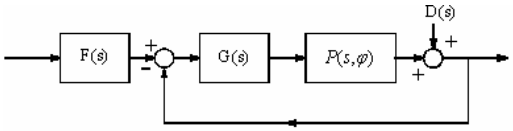

The QFT controller design method is briefly summarised as follows:

- *Step 1:* generation of plant templates prior to the QFT design (at a fixed frequency, the plant's frequency response set is called a *template*).
- *Step 2:* Given the plant templates, QFT converts closed loop magnitude specifications into magnitude constraints on a nominal open- loop function (these are called QFT *bounds*).
- *Step 3:* A nominal open loop function is then designed to simultaneously satisfy its constraints as well as to achieve nominal closed loop stability. In a two DOF design, a pre-filter will be designed after the loop is closed (i.e., after the controller has been designed) (Yaniv, 1998; Amiri Moghadam et al., 2009a).

The objectives of this section are to synthesise suitable controller and pre-filter such that:

First the closed loop system remains stable if the robust margin (the magnitude of closed loop system for all considered uncertainty) is kept less than 1.1.

Second desired robust tracking of the inputs happens if suitable performance of actuator is satisfied using overshoot (=5%) and the settling time (=0.4s) for all plant uncertainty.

At the first step we must define the plant uncertainty (template), which is shown in Figure 21. Then by having robust performance bounds in the loop-shaping phase of design suitable controller and prefilter can be achieve as follows:

$$G = 1.1018 \times \frac{(s+3.522\times10^{6})(s+171.9)(s+1.146)}{(s+2415)(s+491.3)(s+0.0003543)} \tag{18}$$

$$F = \frac{232.6702}{(s+16.53)(s+14.08)} \tag{19}$$

Figure 21 The boundary of the plant templates

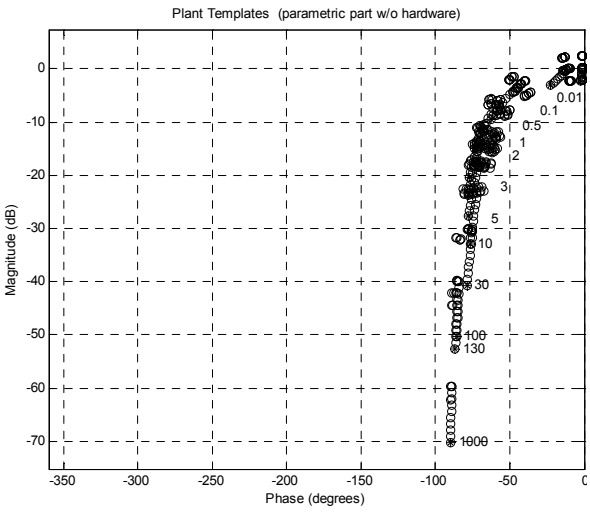

Figure 22 Robust margin bounds

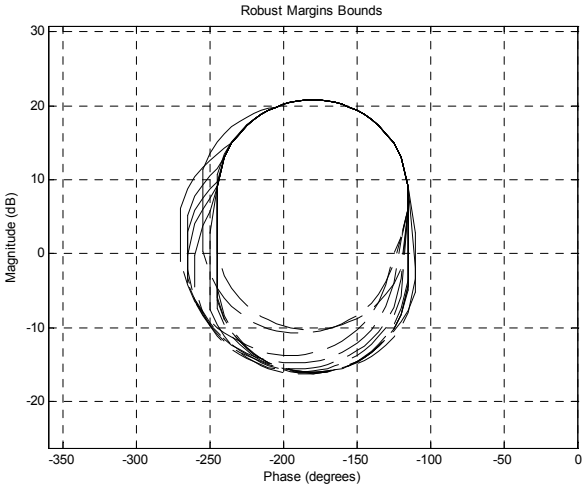

Robust margin bounds are shown in Figure 22. Robust tracking bounds are shown in Figure 23.Figure 24 depicts the loop-shaping of open loop system. It can be observed that the nominal plant exactly lies on its performance bounds which confirm the optimality of design. Figure 25 shows time domain simulation for unit step responses.

Figure 23 Robust tracking bounds

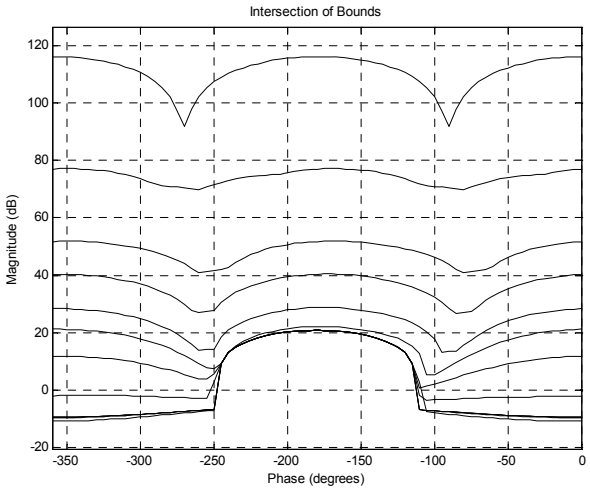

Figure 24 Loop shaping of open-loop system

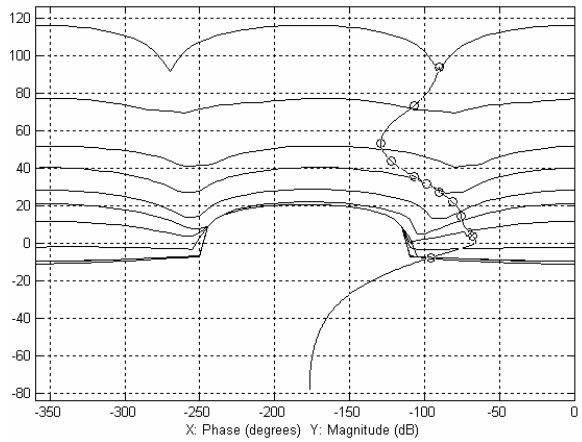

Figure 25 Unit step response for all considered uncertainty with acceptable output bounds

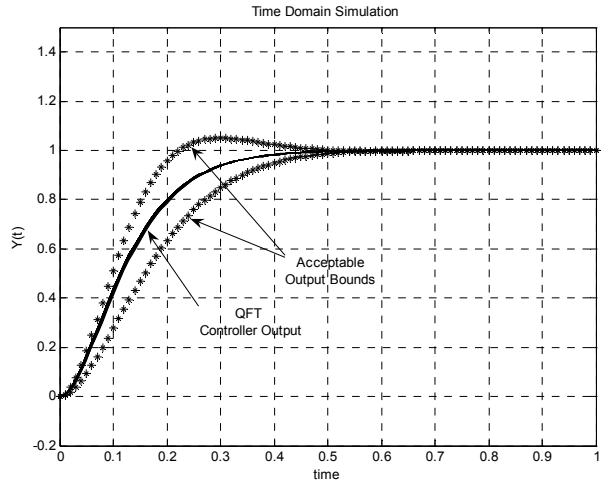

Figure 26 shows the tracking problem for an elliptical trajectory. According to this figure, QFT controller has a good performance for all considered uncertainty of the system.

Figure 26 Tracking problem for an elliptical trajectory (see online version for colours)

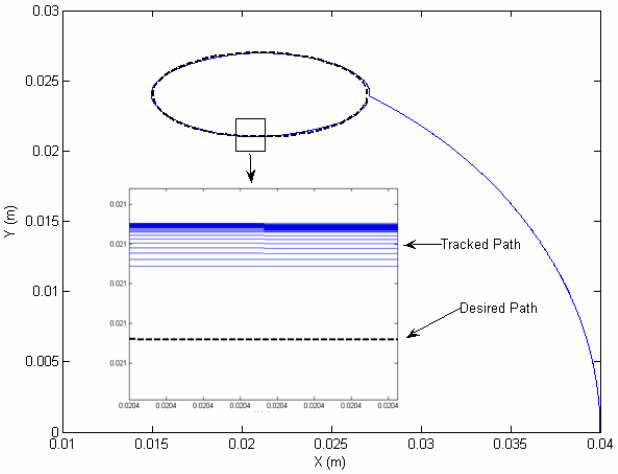

6 Conclusions

In this paper, two major proposals concerning modelling and robust control of a soft robot based on conjugated polymer actuators have been dealt with respectively.

In order to obtain a suitable control oriented dynamic model, Golubev method is used to convert highly uncertain and time-varying dynamics of PPy actuators to a family of Linear Time Invariant systems. This was resulted to improve D.W. Madden's (2000) model capability to predict the actuator uncertainties. ANFIS was applied to solve the inverse kinematics problem.

The robust control QFT was successfully applied to control the soft robot. Moreover, it has been shown that the robot has robust tracking ability and stability under QFT controlling method.

Future work covers

1 development of the mechanical dynamic modelling of conjugated polymer actuator

2 fabrication of a micro robot based on PPy bending actuators.

The research is fortunately ahead of schedule and will be reported soon.

Acknowledgements

This project is partly funded by Research Council of Ferdowsi University of Mashhad. This project is a part of a research programme for achieving a new generation of actuators which can be used in micro and nano robots.

References

Amiri Moghadam, A.A. and Tootoonchi, A.A. (2010) 'Multi-level fuzzy-QFT control of conjugated polymer actuators', *ISR/ROBOTIK*, pp.1038–1045.

Amiri Moghadam, A.A., Gharib, M.R., Moavenian, M. and Torabi, K.Z. (2009a) 'Modelling and control of a SCARA robot using quantitative feedback theory', *Journal of Systems and Control Engineering*, pp.919–928.

Amiri Moghadam, A.A., Moavenian, M. and Torabi, K. (2009b) 'Takagi-Sugeno fuzzy modelling and parallel distribution compensation control of conducting polymer actuators', *Journal of Systems and Control Engineering*, pp.41–51.

Awadallah, M.A. and Soliman, H.M. (2008) 'An adaptive power system stabiliser based on fuzzy and swarm intelligence', *Int. J. of Modelling, Identification and Control*, Vol. 5, pp.55–65.

Bar-Cohen, Y., Xue, T., Shahinpoor, M., Simpson, J. and Smith, J. (1998) 'Flexible, low-mass robotic arm actuated by electroactive polymers and operated equivalently to human arm and hand', *The 3rd Conf. on Robotics for Challenging Environments*, pp.15–21.

Bowers, T.A. (2004) 'Modeling, simulation, and control of a polypyrrole-based conducting polymer actuator', MSc thesis, MIT.

Boxall, D.L. and Osteryoung, R.A. (2004) 'Switching potentials and conductivity of polypyrrole films prepared in the ionic liquid 1-butyl-3-methylimidazolium hexafluorophosphate', *Journal of The Electrochemical Society*, Vol. 151, No. 2, E41.

Della Santa, A., De Rossi, D. and Mazzoldi, A. (1997) 'Characterization and modeling of a conducting polymer muscle-like linear actuator', *Smart Materials and Structures*, Vol. 6, pp.23–34.

Fang, Y. et al. (2008a) 'A scalable model for trilayer conjugated polymer actuators and its experimental validation', *Materials Science and Engineering*, Vol. 28, pp.421–428.

Fang, Y. et al. (2008b) 'Robust adaptive control of conjugated polymer actuators', *IEEE Transactions on Control Systems Technology*, Vol. 16, pp.600–612.

Ge, S.S., Lee, T.H. and Harris, C.J. (1998) 'Adaptive neural networks control of robotic manipulators', *World Scientific Publishing*, Vol. 19.

Golubev, B. and Horowitz, I.M. (1982) 'Plant rational transfer function approximation from input-output data', *International Journal of Control*, Vol. 36, pp.711–723.

Guo, S., Fukuda, T., Kousuge, K., Arai, F., Oguro, K. and Negoro, M. (1995) 'Micro catheter system with active guide wire', *IEEE Int. Conf. on Robotics and Automation*, pp.79–84.

Hollerbach, J.M., Hunter, I.W. and Ballantyne, J. (1992) *A Comparative Analysis of Actuator Technologies for Robotics*, pp.299–342, MIT Press.

Horowitz, I.M. (1992) *Quantitative Feedback Design Theory (QFT)*, Vol. 1, QFT Publications, 4470 Grinnel Ave., Boulder, Colorado 80303, USA.

Horowitz, I.M. and Sidi, M. (1972) 'Synthesis of feedback systems with large plant ignorance for prescribed time domain tolerances', *International Journal of Control*, Vol. 16, pp.287–309.

Houpis, C.H. (1995) 'Quantitative feedback theory (QFT) for the engineer: a paradigm for the design of control systems for uncertain nonlinear plants', Wright Laboratory.

Hunter, I.W. and Lafontaine, S. (1992) 'A comparison of muscle with artificial actuators', *Solid-State Sensor and Actuator Workshop, 5th Technical Digest, IEEE*, pp.178–185.

Jager, E.W.H., Smela, E. and Ingana, O. (2000) 'Microfabricating conjugated polymer actuators', *Science*, Vol. 290, pp.1540–1545.

Jang, J.S.R. (1993) 'ANFIS: adaptive-network-based fuzzy inference system', *IEEE Transactions on Systems Man and Cybernetics*, Vol. 3, pp.665–685.

Jang, J-S.R. and Sun, C-T. (1997) *Neuro-Fuzzy and Soft Computing: A Computational Approach to Learning and Machine Intelligence*, Prentice Hall.

Kaneto, K., Kaneko, M., Min, Y. and MacDiarmid, A.G. (1995) 'Artificial muscle: electromechanical actuators using polyaniline films', *Synthetic Metals*, Vol. 71, pp.2211–2212.

Madden, D.W. (2000) 'Conducting polymer actuators', PhD thesis, MIT.

Madden, P.G.A. (2003) 'Development and modeling of conducting polymer actuators and the fabrication of a conducting polymer based feedback loop', PhD thesis, MIT.

Nakabo, Y., Mukai, T. and Asaka, K. (2005) 'Modeling and visual sensing of multi-DOF robot manipulator with patterned artificial muscle', *IEEE Int. Conf. on Robotics and Automation*, pp.4315–4320.

Otero, T.F. and Sansinena, J.M. (1997) 'Bilayer dimensions and movement inartificial muscles', *Bioelectrochemistry and Bioenergetics*, Vol. 42, pp.117–122.

Singh, J. and Gill, S.S. (2009) 'Fuzzy modelling for burst pressure strength in radial friction welding of GI pipes', *Int. J. of Modelling, Identification and Control*, Vol. 7, pp.305–312.

Smela, E., Inganas, O. and Lundstrom, I. (1995) 'Controlled folding of microsize structures', *Science*, Vol. 268, pp.1735–1738.

Tadokoro, S., Yamagami, S., Ozawa, M., Kimura, T. and Takamori, T. (1999) 'Multi-DOF device for soft micromanipulation consisting of soft gel actuator elements', *IEEE Int. Conf. on Robotics and Automation*, pp.2177–2182.

Torabi, K., Moavenian, Z.M., Amiri, A.A.M. and Amiri, A.H.M. (2009) 'Modelling and control of conjugated polymer actuators using robust control QFT', *17th Annual Int. Conf. on Mechanical Engineering, ISME*, pp.181–190.

Wallace, G. and Spinks, G. (2007) 'Conducting polymers-bridging the bionic interface', *Soft Matter*, Vol. 3, pp.665–671.

Yaniv, O. (1998) *Quantitative Feedback Design of Linear and Non-linear Control Systems*, Kluwer Academic Publication, Norwell, Massachussets.